Available online at www.sciencedirect.com
ScienceDirect
International Journal of Heat and Mass Transfer 50 (2007) 2503–2513
International Journal of HEAT and MASS TRANSFER
www.elsevier.com/locate/ijhmt

Estimation of spray cooling characteristics on a hot surface using the hybrid inverse scheme

Han-Taw Chen *, Hung-Chih Lee

Department of Mechanical Engineering, National Cheng Kung University, Tainan City 701, Taiwan

Received 22 July 2006; received in revised form 1 December 2006

Abstract

A hybrid technique of the Laplace transform and finite-difference methods in conjunction with the least-squares method and experimental temperature data inside the test material is applied to investigate the spray cooling of a hot surface. In this study, the unknown surface temperature and heat flux will be predicted. Their functional forms are unknown a priori in the present study and are assumed to be the functions of time before performing the inverse calculation. The whole time domain is divided into several analysis sub-time intervals and then these unknown estimates on each analysis interval can be predicted. In order to validate the accuracy of the present inverse method, comparisons between the present estimates and previous estimated results are made. The results show that the present estimates of the unknown temperature at various measurement locations agree with the previous estimated results and experimental temperature data. However, the present estimates of the unknown surface heat flux deviate from the previous estimated results for larger times.

1. Introduction

Spray cooling has received much attention in recent years because it can remove high heat fluxes. Typical applications were found in a wide range of industrial processes such as rapid cooling and quenching in metal foundries, cooling of electronics components, nuclear power generation and the use of high power lasers, etc. The metallurgical industry often used spray cooling for quenching of iron ingots and cooling of alloy strips in continuous casting processes. It is well known that the surface temperature of the test hot surface was the most important parameter in quenching and was used to define four distinct heat transfer regimes of the boiling curve: (1) film boiling, (2) transition boiling, (3) nucleate boiling and (4) single phase liquid cooling.

Qiao and Chandra [1] stated that adding a surfactant to water sprays can enhance nucleate boiling during spray cooling, and the surface heat transfer rate can be increased by up to 300% for surface temperatures between 100 °C and 120 °C. Jia and Qiu [2] applied spray cooling experiments with pure water and water solution of 100 ppm solution of surfactant to measure droplet characteristics, surface heat flux and surface temperature. Cui et al. [3] experimentally investigated the effect of dissolving salts in water sprays used for quenching a hot copper surface. The variation of the surface temperature with the spray cooling time during spray quenching was recorded, and the surface heat flux was calculated from the temperature measurements using the sequential function specification method. Qiao and Chandra [1] and Cui et al. [3] applied the sequential function specification method to estimate the surface heat flux. However, Cui et al. [3] did not show how to determine the surface heat flux in detail. Hsieh et al. [4] applied the transient liquid crystal technique and thermocouple to determine the variation of the surface temperature with time during spray cooling of a hot surface for pure water and R-134a. The surface heat flux can be obtained from semi-infinite heat conduction problem. Cooling curves were obtained for different spray mass flux,

* Corresponding author. Fax: +886 6 235 2973.
E-mail address: htchen@mail.ncku.edu.tw (H.-T. Chen).

0017-9310/$ - see front matter © 2007 Elsevier Ltd. All rights reserved.
doi:10.1016/j.ijheatmasstransfer.2006.12.021

Nomenclature

C_j	undetermined coefficient
$F_1(t)$	unknown function
$[F]$	force matrix
$[K]$	global conduction matrix
L	thickness of the test material, m
ℓ	distance between two neighboring nodes, m
M	number of the discrete measurement times
M_t	number of the discrete times
m_1	spray mass flux, kg/m^2 s
n	total number of nodes
P	number of the sub-time intervals
s	Laplace transform parameter
T	temperature, °C
$\widetilde{T}$	temperature in the transform domain
$\{\widetilde{T}\}$	global matrix of the nodal temperatures in the transform domain
T_{in}	initial temperature, °C
$T_L(t)$	given temperature measurement at $x = L$, °C
t	time, s
Δt_e	measurement time step, $(t_f - t_0)/(M_t - 1)$
t_f	final time, s
t_0	initial measurement time, s
t_r	discrete measurement time, s
U_m	mean droplet impact velocity, m/s
x	spatial coordinate, m
x_m	location of the thermocouple

Greeks symbols

α	referenced thermal diffusivity, m^2/s
ε	prescribed accuracy

Subscripts

cal	calculated value
est	estimated value
mea	measured data

Weber number and degrees of superheat and subcooling. However, the unknown heat transfer coefficient was assumed to be constant in their work [4].

The accurate estimations of the surface heat flux and temperature are significant during spray cooling of a hot surface. It is known that the estimations of the surface temperature and heat flux from the measured temperatures inside the test material can be regarded as the inverse heat conduction problems (IHCP). The IHCP are often regarded as the ill-posed problem because their solution does not satisfy the general requirements of existence, uniqueness and stability under small changes to the input data. The main difficulty of the IHCP is that their solution is very sensitive to changes in input data resulting from measurement errors [5–7]. It can be found that various inverse methods, such as the implicit finite-difference, regularization, conjugate gradient, function specification, Kalman filter and hybrid scheme methods have been developed for solving the IHCP [5–7]. Su and Hewitt [8] used the Alifanov's iterative regulation method to estimate the time-varying heat transfer coefficient of forced-convective flow boiling over the outer surface of a heater tube with 8.965 mm in the inner radius and 9.525 mm in the outer radius. Ji and Jang [9] applied the Kalman filter technique in conjunction with the actual measured temperatures to predict the unknown surface heat flux across a 1-mm-thick copper plate. Their estimated value of the surface heat flux was not in good agreement with the measured heat flux for various peak waves and exhibited the oscillatory phenomenon. Kim et al. [10] estimated the time- and space-varying heat flux on the surface of a three-dimensional slab with temperature-dependent thermophysical properties using the sequential gradient method combined with a cubic-spline function specification. Their estimates of the time-varying heat flux at the center deviated from the exact solution.

Most numerical schemes for the IHCP may be sensitive to measurement noise. This sensitivity often depends on the time-step. In general, the smaller the time-step is, the more ill-posed the problem is. In order to overcome this drawback, Chen and Chang [11] first introduced a hybrid scheme of the Laplace transform and finite-difference methods to estimate the unknown surface temperature in one-dimensional IHCP using the measured nodal temperatures inside the test material without measurement errors. Later, Chen et al. [12–15] applied the similar scheme in conjunction with a sequential-in-time concept and the least-squares method to estimate the unknown surface boundary conditions from the measured temperatures or measured displacements with measurement errors. The results showed that the estimates of the unknown surface boundary conditions were in good agreement with the direct results for the cases without measurement errors. In addition, the effects of the measurement time-step and measurement locations on the estimates were not very sensitive for this hybrid method [12–15]. The present estimates did not exhibit the severe oscillatory phenomenon and large deviation from the direct results for the cases with measurement errors. Thus the present study further applies this hybrid inverse scheme in conjunction with experimental temperature data given by Qiao and Chandra [1] and Cui et al. [3] to estimate the unknown surface temperature and heat flux during spray cooling. Then, comparisons of the unknown surface temperature and heat flux between the present estimates and those given by Qiao and Chandra [1] and Cui et al. [3] are made.

2. Mathematical formulation

A one-dimensional heat conduction problem can be introduced to estimate the unknown surface temperature and heat flux during spray cooling. The physical geometry of the present problem is shown in Fig. 1. The mathematical formulation, basic assumptions and experimental temperature data used in this study come from the works of Qiao and Chandra [1] and Cui et al. [3]. For the direct heat conduction problems, the temperature field can be determined provided that the boundary conditions at $x = 0$ and $x = L$ are given. However, one of the boundary conditions is unknown for the inverse heat conduction problems. It cannot be estimated unless additional information on the temperature history in the test material is given. In this study, the thermocouple is welded at $x = x_m$ in order to record the temperature history during spray cooling. The IHCP investigated here involve the estimates of the unknown surface heat flux and temperature from the transient temperature measurements at $x = x_m$. The governing differential equation, boundary conditions and initial condition are expressed as

$$k\frac{\partial^2 T}{\partial x^2} = \rho c\frac{\partial T}{\partial t} \quad 0 < x < L, \quad 0 < t \leqslant t_f \tag{1}$$

$$T(L,t) = T_L(t) \tag{2}$$

$$T(0,t) = F_1(t) = ? \tag{3}$$

and

$$T(x,0) = T_{in} \tag{4}$$

where T is the temperature. t and x respectively denote time and spatial-domain variables. k is the thermal conductivity of the test material. ρ is the density. c is the specific heat. $T_L(t)$ is the given temperature measurement. T_{in} is the initial temperature. t_f denotes the time that spray cooling was terminated. The unknown surface temperature $F_1(t)$ can be estimated provided that the knowledge of transient temperature reading at $x = x_m$ is given.

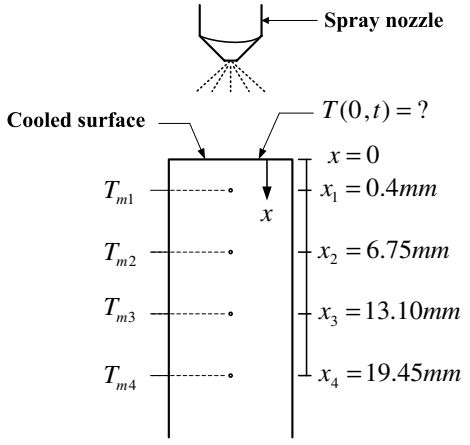

Fig. 1. Physical geometry for the temperature measurements of a hot plate during spray cooling.

A curve-fitted profile generated through a least-squares process can be used to fit experimental temperature data. Later, the history of the measured temperature $T^{mea}(x_m, t)$ is obtained from this curve-fitted profile.

3. Numerical analysis

In order to remove the time-dependent terms from the governing differential equation and boundary conditions, the method of the Laplace transform is employed. The Laplace transforms of Eqs. (1)–(3) with respect to t in conjunction with the initial condition (4) give

$$\frac{\partial^2 \widetilde{T}}{\partial x^2} - \frac{s}{\alpha}\widetilde{T} = -\frac{T_{in}}{\alpha}, \quad 0 < x < L \tag{5}$$

and

$$\widetilde{T}(0) = \widetilde{F}_1 \quad \text{at } x = 0 \tag{6}$$

$$\widetilde{T}(L) = \widetilde{T}_L \quad \text{at } x = L \tag{7}$$

where $\alpha = \frac{k}{\rho c}$ is the thermal diffusivity and s is the Laplace transform parameter. $\widetilde{T}$ is defined as

$$\widetilde{T}(x,s) = \int_0^\infty e^{-st} T(x,t)\,dt \tag{8}$$

The application of the central-difference approximation to Eq. (5) can obtain the following discretized form as

$$\frac{\widetilde{T}_{i+1} - 2\widetilde{T}_i + \widetilde{T}_{i-1}}{\ell^2} - \frac{s}{\alpha}\widetilde{T}_i = -\frac{T_{in}}{\alpha} \quad \text{for } i = 2,3,\ldots,n-1 \tag{9}$$

where n is the nodal number. $\ell = L/(n-1)$ denotes the distance between two neighboring nodes and is uniform.

The discretized forms at $x = 0$ and $x = L$ are expressed as

$$\widetilde{T}_1 = \widetilde{F}_1 \tag{10}$$

and

$$\widetilde{T}_n = \widetilde{T}_L \tag{11}$$

The arrangement of Eq. (9) in conjunction with the discretized forms of its corresponding boundary conditions (10) and (11) yields the following matrix equation.

$$[K][\widetilde{T}] = [F] \tag{12}$$

where $[K]$ is a matrix with the parameter s. $[\widetilde{T}]$ is a matrix representing the unknown nodal temperatures in the transform domain. $[F]$ is a matrix representing the forcing term. The direct Gauss elimination algorithm and the numerical inversion of the Laplace transform [16] are applied to solve Eq. (12) in order to determine the nodal temperatures at a specific time. One of the advantages of the present method is that the unknown estimates do not always need to proceed with step-by-step computation from the initial time $t = 0$.

The functional form of the unknown surface temperature $F_1(t)$ in the present study is assumed to be the function of time before performing the inverse calculation. However, it is not easy to obtain an approximate polynomial function that can completely fit $F_1(t)$ for the whole time domain considered. Under this circumstance, a sequential-in-time procedure is introduced to estimate $F_1(t)$. In other words, the whole time domain $t_0 \leqslant t \leqslant t_f$ will be divided into p sub-time intervals. The unknown surface temperature $F_1(t)$ on each sub-time interval can be approximated by an $(N-1)$th degree polynomial guess function of time and is expressed as

$$F_1(t) = \sum_{j=1}^{N} C_j t^{j-1} \tag{13}$$

where C_j, $j = 1, 2, \ldots, N$, are the unknown coefficients and can be estimated using the least-squares method in conjunction with the measured temperatures on each analysis interval.

The least-squares minimization technique is applied to minimize the sum of the squares of the deviations between the calculated temperature $T^{\mathrm{cal}}(x_m, t_r)$ and measured temperature $T^{\mathrm{mea}}(x_m, t_r)$ at a sensor location x_m, where t_r is the discrete measurement time and can be written as $t_r = t_0 + r\Delta t_e, \quad r = 0, 1, \ldots, M_t - 1. \quad M_t = p(N-1) + 1$ denotes the number of the discrete measurement times. Δt_e is the measurement time step and is defined as $\Delta t_e = (t_f - t_0)/(M_t - 1)$. The error in the estimates $E(C_1, C_2, \ldots, C_N)$ on each analysis interval $t_i \leqslant t_r \leqslant t_{i+N-1}$, $i = 0, N-1, 2(N-1), \ldots, M_t - N$, can be expressed as

$$E(C_1, C_2, \ldots, C_N) = \sum_{r=i}^{i+N-1} \left[T^{\mathrm{cal}}(x_m, t_r) - T^{\mathrm{mea}}(x_m, t_r)\right]^2 \tag{14}$$

Due to the application of the Laplace transform, t_0 is not always the initial time $t = 0$ in the present inverse scheme. The estimated values of $C_j, j = 1, 2, \ldots, N$, are determined provided that the values of $E(C_1, C_2, \ldots, C_N)$ are minimum. The computational procedures for estimating the unknown coefficients $C_j, j = 1, 2, \ldots, N$, are described as follows.

First, the initial guesses of $C_j, j = 1, 2, \ldots, N$, are chosen. Later, the calculated temperature at $x = x_m$, $T^{\mathrm{cal}}(x_m, t_r)$, can be determined from Eq. (12). Deviations of $T^{\mathrm{cal}}(x_m, t_r)$ and $T^{\mathrm{mea}}(x_m, t_r)$ on each analysis interval $t_i \leqslant t_r \leqslant t_{i+N-1}, \quad i = 0, N-1, 2(N-1), \ldots, M_t - N,$ are expressed as

$$e_p = T^{\mathrm{cal}}(x_m, t_r) - T^{\mathrm{mea}}(x_m, t_r) \quad \text{for } p = r - i + 1, i \leqslant r \leqslant i + N - 1 \tag{15}$$

The new calculated value $T^{\mathrm{cal},p}(x_m, t_r)$ on each analysis interval $t_i \leqslant t_r \leqslant t_{i+N-1}, \quad i = 0, N-1, 2(N-1), \ldots, M_t - N$, can be expanded in the first-order Taylor's series approximation as

$$T^{\mathrm{cal},p}(x_m, t_r) = T^{\mathrm{cal}}(x_m, t_r) + \sum_{j=1}^{N} \frac{\partial T^{\mathrm{cal}}}{\partial C_j} \mathrm{d}C_j \quad \text{for } p = r - i + 1, i \leqslant r \leqslant i + N - 1 \tag{16}$$

In order to obtain the derivative $\frac{\partial T^{\mathrm{cal}}}{\partial C_j}$ in Eq. (16), the new unknown coefficient C_j^* is introduced as

$$C_j^* = C_j + d_j \delta_{jk} \quad \text{for } j, k = 1, 2, \ldots, N \tag{17}$$

where $d_j = C_j^* - C_j$ is a small value corresponding to C_j. The symbol δ_{jk} is Kronecker delta.

Similarly, the new calculated value $T^{\mathrm{cal},p}(x_m, t_r)$ with respect to C_j^* can also be determined from Eq. (12). Deviations between $T^{\mathrm{cal},p}(x_m, t_r)$ and $T^{\mathrm{mea}}(x_m, t_r)$ on each analysis interval $t_i \leqslant t_r \leqslant t_{i+N-1}$, $i = 0, N-1, 2(N-1), \ldots, M_t - N$, can be written as

$$e_j^p = T^{\mathrm{cal},p}(x_m, t_r) - T^{\mathrm{mea}}(x_m, t_r) \quad \text{for } j, p = 1, 2, \ldots, N \tag{18}$$

The finite-difference representation of the derivative $\frac{\partial T^{\mathrm{cal}}}{\partial C_j}$ is expressed as

$$\omega_j^p = \frac{\partial T^{\mathrm{cal}}}{\partial C_j} = \frac{T^{\mathrm{cal},p} - T^{\mathrm{cal}}}{C_j^* - C_j} \quad \text{for } j, p = 1, 2, \ldots, N \tag{19}$$

The substitution of Eqs. (15), (17) and (18) into Eq. (19) yields

$$\omega_j^p = (e_j^p - e_p)/d_j \tag{20}$$

Substituting Eq. (19) into Eq. (16) yields

$$T^{\mathrm{cal},p}(x_m, t_r) = T^{\mathrm{cal}}(x_m, t_r) + \sum_{j=1}^{N} \omega_j^p d_j^* \quad \text{for } p = r - i + 1, i \leqslant r \leqslant i + N - 1 \tag{21}$$

where $d_j^* = \mathrm{d}C_j$ denotes the new correction of C_j.

Substituting Eqs. (15) and (18) into Eq. (21) yields

$$e_j^p = e_p + \sum_{j=1}^{N} \omega_j^p d_j^* \quad \text{for } p = 1, 2, \ldots, N \tag{22}$$

In accordance with Eqs. (14) and (18), the error in the estimates $E(C_1 + \Delta C_1, C_2 + \Delta C_2, \ldots, C_N + \Delta C_N)$ can be expressed as

$$E = \sum_{p=1}^{N} (e_j^p)^2 \tag{23}$$

In order to yield the minimum value of E with respect to C_j, differentiating E corresponding to the new corrections d_j^* is performed. Thus the correction equations corresponding to $C_j$can be expressed as

$$\sum_{j=1}^{N} \sum_{p=1}^{N} \omega_p^k \omega_p^j d_j^* = -\sum_{p=1}^{N} \omega_k^p e_p \quad \text{for } k = 1, 2, \ldots, N \tag{24}$$

Eq. (24) is a set of N algebraic equations for the new corrections d_j^*, $j = 1, 2, \ldots, N$. The new corrections d_j^*,

$j = 1, 2, \ldots, N$, are obtained from this equation. Later, $C_j + d_j^*$ can be determined and is regarded as the new guessed coefficient of C_j. The above numerical procedures are repeated until the values of $\left|\frac{T^{\text{cal}}(x_m,t_r)-T^{\text{mea}}(x_m,t_r)}{T^{\text{mea}}(x_m,t_r)}\right|$ on each analysis interval $t_i \leqslant t_r \leqslant t_{i+N-1}$, $i = 0, N-1, 2(N-1), \ldots, M_t - N$, are all less than a prescribed accuracy ε. In the present study, $\varepsilon = 0.0001$ is taken through all the cases.

Once the unknown surface temperature is obtained, the temperature distribution at a specified time is obtained using the direct method. The unknown surface heat flux $q^{\text{est}}(0,t)$ can be determined from the following expression [6].

$$q^{\text{est}}(0,t) = -k\left.\frac{\partial T}{\partial x}\right|_{x=0} = -k\frac{4T_2 - 3T_1 - T_3}{2\ell} \tag{25}$$

4. Results and discussion

In order to demonstrate the accuracy and reliability of the present inverse scheme, two experimental examples given by Qiao and Chandra [1] and Cui et al. [3] are illustrated. Comparisons between the present estimates and their estimated results and experimental data [1,3] are also made. All the computations of the illustrated examples are performed on a PC.

Example 1. A schematic diagram of the apparatus built used for spraying cooling experiments was shown in Fig. 1 of Ref. [1]. The spray nozzle and test surface were enclosed in an aluminum chamber. The cooled surface was the flat face of a 25.4 mm diameter copper cylinder which was electroplated with a 10 μm thick layer of nickel to prevent oxidation. The main components of this system were a water delivery system, a spray nozzle, a heated copper cylinder, a data acquisition and control system to record the surface temperature. However, the governing differential equation, boundary conditions, initial condition and some thermophysical quantities of the heated copper cylinder were not shown in the work of Qiao and Chandra [1]. Qiao and Chandra [1] applied the sequential function specification method [7] to estimate the unknown surface heat flux $q(0,t)$ and temperature $T(0,t)$ during spray quenching. The following thermophysical quantities are taken from Ref. [17] for inverse analysis of Example 1. These thermophysical quantities are $\rho = 8933\ \text{kg/m}^3$, $k = 385.1\ \text{W/(m °C)}$, $c = 412.66\ \text{J/(kg °C)}$ and $T_{\text{in}} = 240\ °\text{C}$. The main purpose of the present study is to apply experimental data at four different measurement locations given by Qiao and Chandra [1] to estimate the unknown surface temperature and heat flux during spraying cooling. Furthermore, comparisons of the unknown surface temperature and heat flux between the present estimates and those given by Qiao and Chandra [1] are also made.

Qiao and Chandra [1] applied four 0.5 mm diameter K-type (chromel–alumel) thermocouples to measure temperatures of the test cylinder at x_1, x_2, x_3 and x_4, where x_1, x_2, x_3 and x_4 denote these four different measurement locations. These four thermocouples were inserted into holes drilled 6.35 mm apart along the axis of the copper cylinder. However, the first thermocouple was positioned at 0.4 mm below the cooled surface of the test cylinder. This implies that x_1, x_2, x_3 and x_4 respectively are $x_1 = 0.4$ mm, $x_2 = 6.75$ mm, $x_3 = 13.1$ mm and $x_4 = 19.85$ mm. The holes were filled with a high thermal conductivity paste before inserting the thermocouples to minimize the thermal contact resistance. Measured temperatures were continuously recorded using a digital data acquisition system. The histories of the measured temperatures at $x = x_1, x_2, x_3$ and x_4 during spray cooling with pure water, a spray mass flux $m_1 = 0.5\ \text{kg/m}^2\,\text{s}$ and a mean droplet impact velocity $U_m = 20\ \text{m/s}$ are shown in Fig. 4. of Ref. [1] and Fig. 2. The least-squares fitting method is applied to fit these four experimental temperature data over the whole time domain. The functional expressions of these measured temperatures are expressed as follows:

$$T^{\text{mea}}(x_1,t) = \begin{cases} 239.586 - 1.25t + 0.146t^2 - 1.213\times10^{-2}t^3 \\ \quad +5.353\times10^{-4}t^4 - 1.327\times10^{-5}t^5 \\ \quad +1.844\times10^{-7}t^6 - 1.331\times10^{-9}t^7 \\ \quad +3.837\times10^{-12}t^8 \quad \text{for } 0 \leqslant t \leqslant 80\ \text{s} \\ -2.641\times10^{4} + 1.443\times10^{3}t - 30.744t^2 \\ \quad +0.322\times10^{-2}t^3 - 1.666\times10^{-3}t^4 \\ \quad +3.41\times10^{-6}t^5 \quad \text{for } 80\ \text{s} < t \leqslant 115\ \text{s} \end{cases} \tag{26}$$

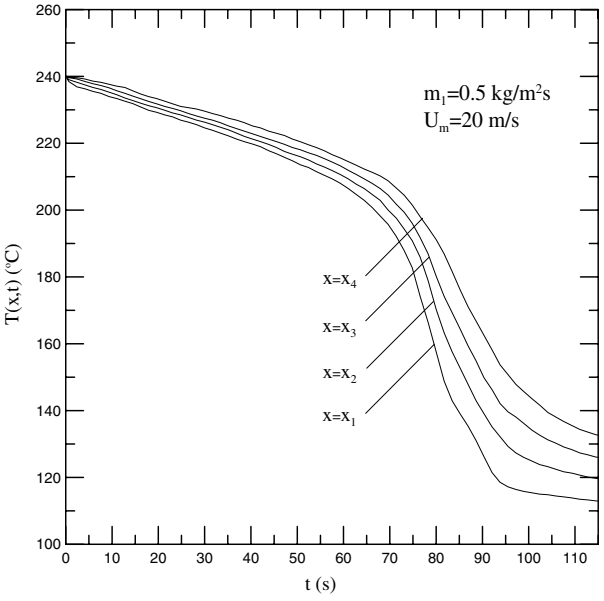

Fig. 2. Experimental temperature data at various measurement locations given by Qiao and Chandra [1] for $m_1 = 0.5\ \text{kg/(m}^2\,\text{s)}$ and $U_m = 20\ \text{m/s}$.

$$T^{\mathrm{mea}}(x_2,t)=\begin{cases}239.774-0.681t+3.832\times10^{-2}t^2\\ \quad -2.865\times10^{-3}t^3+1.13\times10^{-4}t^4\\ \quad -2.394\times10^{-6}t^5+2.56\times10^{-8}t^6\\ \quad -1.091\times10^{-10}t^7 \quad \text{for } 0\leqslant t\leqslant 80\text{ s}\\ -13370+734.094t-15.4678t^2+0.159t^3\\ \quad -8.066\times10^{-4}t^4+1.612\times10^{-6}t^5\\ \quad \text{for } 80\text{ s}<t\leqslant 115\text{ s}\end{cases}\tag{27}$$

$$T^{\mathrm{mea}}(x_3,t)=\begin{cases}239.959-0.332t+2.95\times10^{-3}t^2\\ \quad -4.459\times10^{-4}t^3+3.439\times10^{-5}t^4\\ \quad -9.519\times10^{-7}t^5+1.176\times10^{-8}t^6\\ \quad -5.52\times10^{-11}t^7 \quad \text{for } 0\leqslant t\leqslant 80\text{ s}\\ 4.678\times10^{5}-3.427\times10^{4}t+1071t^2-18.478t^3\\ \quad +0.19t^4-1.167\times10^{-3}t^5+3.959\times10^{-6}t^6\\ \quad -5.722\times10^{-9}t^7 \quad \text{for } 80\text{ s}<t\leqslant 115\text{ s}\end{cases}\tag{28}$$

and

$$T^{\mathrm{mea}}(x_4,t)=\begin{cases}239.808+5.975\times10^{-2}t-4.997\times10^{-2}t^2\\ \quad +2.421\times10^{-3}t^3-5.692\times10^{-5}t^4\\ \quad +6.159\times10^{-7}t^5-2.146\times10^{-9}t^6\\ \quad -4.756\times10^{-12}t^7 \quad \text{for } 0\leqslant t\leqslant 80\text{ s}\\ -2.039\times10^{4}+952.7t-16.004t^2\\ \quad +0.103t^3+7.207\times10^{-5}t^4\\ \quad -3.676\times10^{-6}t^5+1.169\times10^{-8}t^6\\ \quad \text{for } 80\text{ s}<t\leqslant 115\text{ s}\end{cases}\tag{29}$$

The unknown coefficients $C_j, j=1,2,3$, used to begin the iteration are taken as unity. A second-degree polynomial guess function ($N=3$) is selected to approximate the history of the unknown surface temperature $T(0,t)$ on each sub-time interval. Then the nodal temperatures $T_2(t)$ and $T_3(t)$ can be determined from Eq. (12) using the obtained surface temperature $T(0,t)$. Further, the unknown surface heat flux $q(0,t)$ can be obtained from Eq. (25). In order to validate the accuracy and reliability of the present estimates, the present study applies two different L values to predict $T(0,t)$ and $q(0,t)$. Figs. 3 and 4 respectively show the comparisons of $T(0,t)$ and $q(0,t)$ between the present estimates and those given by Qiao and Chandra [1] for $m_1=0.5\ \mathrm{kg/(m^2\,s)}$, $U_m=20\ \mathrm{m/s}$, $M=22$, $x_m=x_1$, $\ell=0.05$ mm and various L values. The results show that the present estimate of the unknown surface temperature $T(0,t)$ using $L=13.1$ mm and 19.45 mm agrees well with the estimated result of Qiao and Chandra [1]. However, the present estimate of $q(0,t)$ slightly deviates from the estimated result of Qiao and Chandra [1] for $0\leqq t\leqq 75$ s. Later, their deviation gradually increases with time for $75\text{ s}<t\leqq 110$ s. The maximum error between the present estimate and the estimated result of Qiao and Chandra [1] can occur at the final time $t=110$ s and is up to 3.5 times. It can be found from Fig. 4 that the present estimate of $q(0,t)$ using $L=13.1$ mm is also in good agreement with that using $L=19.45$ mm. The present estimates

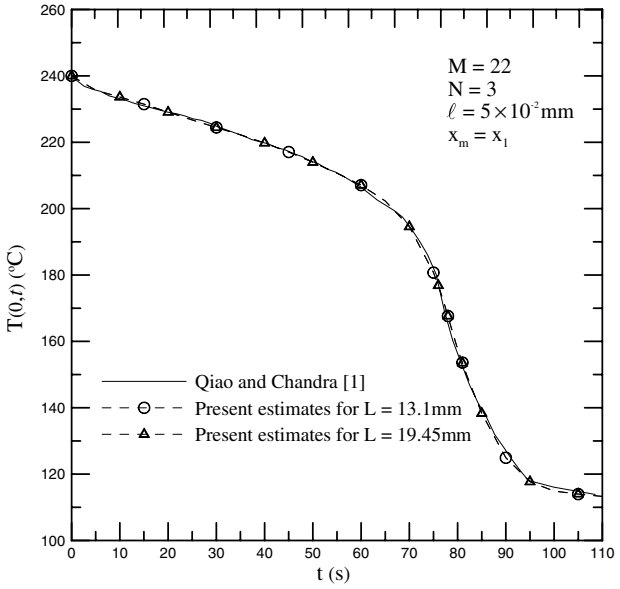

Fig. 3. Comparison of $T(0,t)$ between the present estimates and those given by Qiao and Chandra [1] for $m_1=0.5\ \mathrm{kg/(m^2\,s)}$, $U_m=20\ \mathrm{m/s}$ and various L values.

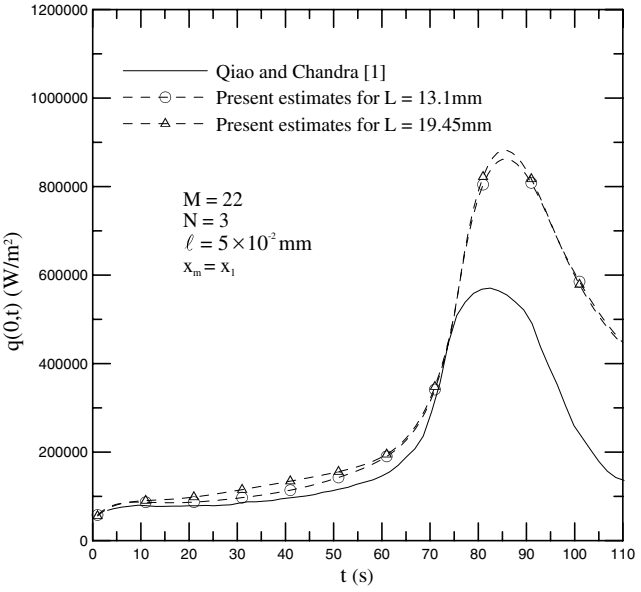

Fig. 4. Comparison of $q(0,t)$ between the present estimates and those given by Qiao and Chandra [1] for $m_1=0.5\ \mathrm{kg/(m^2\,s)}$, $U_m=20\ \mathrm{m/s}$ and $L=13.1$ mm.

and the predicted results of Qiao and Chandra [1] both show that the peak values of the surface heat flux $q(0,t)$ occur about at $t=84$ s. However, the present estimates of $q(0,t)$ for $L=13.1$ mm and 19.45 mm both are higher than those given by Qiao and Chandra [1] especially for $75\text{ s}<t\leqq 110$ s. Once the history of the unknown surface heat flux $q(0,t)$ is obtained, $T(x_2,t)$ can be obtained using the present direct scheme. In order to validate the accuracy of $q(0,t)$ further, this predicted result is applied to determine $T(0,t)$ and $T(x_2,t)$. The comparisons of $T(0,t)$ and

$T(x_2,t)$ between the direct results using two given estimates of $q(0,t)$ and experimental temperature data given by Qiao and Chandra [1] are made, as shown in Figs. 5 and 6. It can be observed from Figs. 5 and 6 that the present direct results of $T(0,t)$ and $T(x_2,t)$ using the present estimate of $q(0,t)$ agree well with experimental temperature data given by Qiao and Chandra [1] for $0 \leqq t \leqq 110$ s. However, the deviations between experimental temperature data and the direct results of $T(0,t)$ and $T(x_2,t)$ using the given estimate of $q(0,t)$ given by Qiao and Chandra [1] are small for $0 \leqq t \leqq 75$ s and gradually increases with time for 75 s $< t \leqq 110$ s. This implies that the present estimates are accurate and reliable.

In order to investigate the effect of the measurement locations on the present estimates, Figs. 7 and 8 respectively show the comparisons of $T(0,t)$ and $q(0,t)$ between the present estimates and those given by Qiao and Chandra [1] for $m_1 = 0.5$ kg/m^2 s, $U_m = 20$ m/s, $L = 13.1$ mm and various measurement locations. The results show that the deviation of the present estimates obtained from $x_m = x_1$

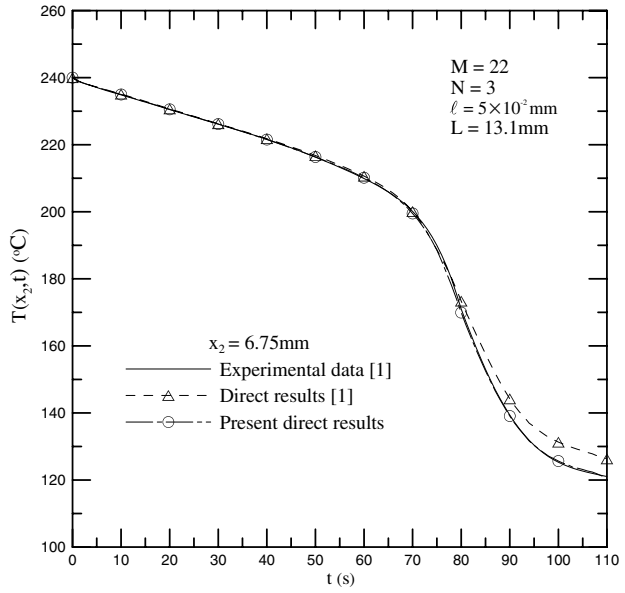

Fig. 5. Comparison of $T(x_2,t)$ between the direct results using two given estimates of $q(0,t)$ and experimental data given by Qiao and Chandra [1] for $m_1 = 0.5$ kg/(m^2 s), $U_m = 20$ m/s and $L = 13.1$ mm.

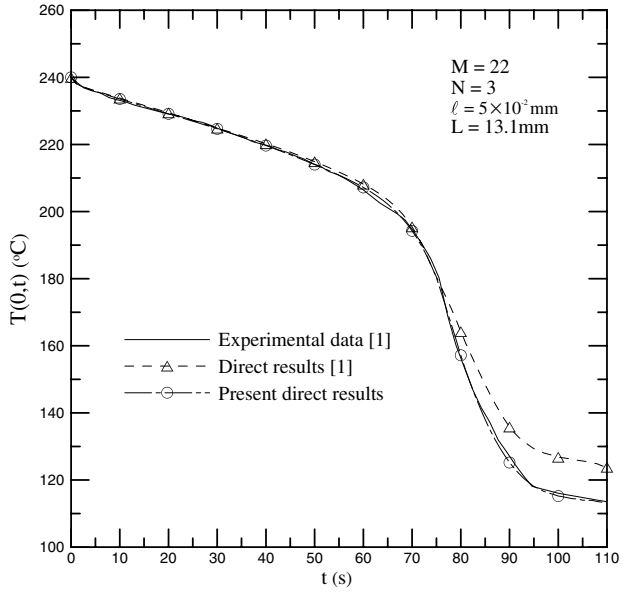

Fig. 6. Comparison of $T(0,t)$ between the direct results using two given estimates of $q(0,t)$ and experimental data given by Qiao and Chandra [1] for $m_1 = 0.5$ kg/(m^2 s), $U_m = 20$ m/s and $L = 13.1$ mm.

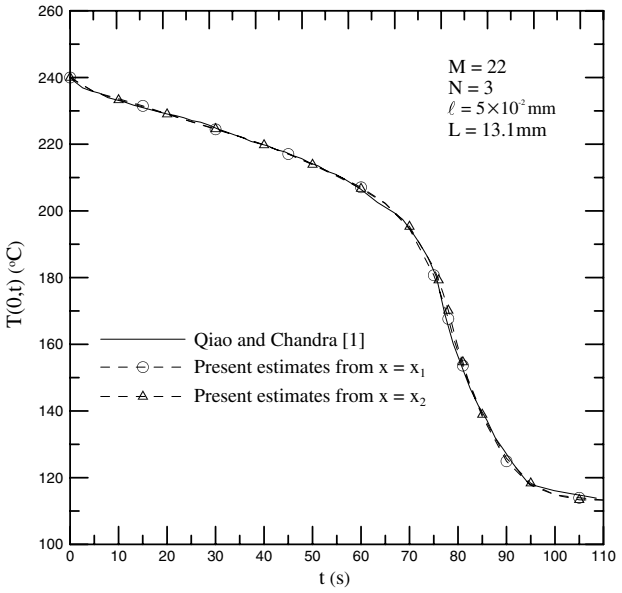

Fig. 7. Comparison of $T(0,t)$ between the present estimates and those given by Qiao and Chandra [1] for $m_1 = 0.5$ kg/(m^2 s), $U_m = 20$ m/s, $L = 13.1$ mm and various measurement locations.

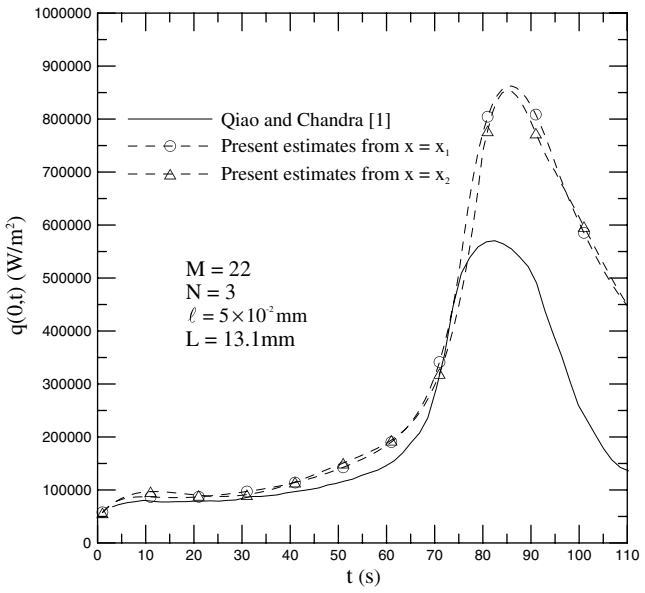

Fig. 8. Comparison of $q(0,t)$ between the present estimates and those given by Qiao and Chandra [1] for $m_1 = 0.5$ kg/(m^2 s), $U_m = 20$ m/s, $L = 13.1$ mm and various measurement locations.

and $x_m = x_2$ is small. This implies that the present estimates are not very sensitive to the measurement location.

Example 2. A schematic diagram of the apparatus built to measure the surface temperature during spraying cooling was shown in Fig. 1 of Ref. [3]. This apparatus was a modified version of the one designed by Qiao and Chandra [1]. The main components of this system were a water delivery system, a spray nozzle, a heated copper test surface, a data acquisition and control system to record the surface temperature. Similarly, the governing differential equation, boundary conditions, initial condition and some thermophysical quantities were not shown in their work [3]. In order to compare with the predicted results of the surface temperature and heat flux given by them [3], it is found that the material of the heated test cylinder seems to be brass not copper. The following thermophysical quantities are taken from Ref. [17] for inverse analysis of this example: $\rho = 8530\ \text{kg/m}^3$, $k = 144.4\ \text{W/(m °C)}$, $c = 412.0\ \text{J/(kg °C)}$ and $T_{\text{in}} = 240\ °\text{C}$. The present study also applies experimental temperature data at x_1, x_2, x_3 and x_4 given by Cui et al. [3] to estimate the unknown surface temperature and heat flux during spraying cooling. Furthermore, comparisons of the unknown surface temperature and heat flux between the present estimates and those given by Cui et al. [3] are also made.

Cui et al. [3] also applied four 0.5 mm diameter K-type (chromel–alumel) thermocouples to measure temperatures of the test cylinder at x_1, x_2, x_3 and x_4. As shown in Example 1, x_1, x_2, x_3 and x_4 respectively are $x_1 = 0.4$ mm, $x_2 = 6.75$ mm, $x_3 = 13.1$ mm and $x_4 = 19.85$ mm. Measured temperatures were continuously recorded using a digital data acquisition system. The histories of the measured temperatures at $x = x_1$, x_2, x_3 and x_4 are shown in Fig. 2 of Ref. [3] and Fig. 9. The least-squares fitting method is applied to fit the histories of four experimental temperature data at $x = x_1$, x_2, x_3 and x_4. The functional expressions of these measured temperatures are expressed as follows:

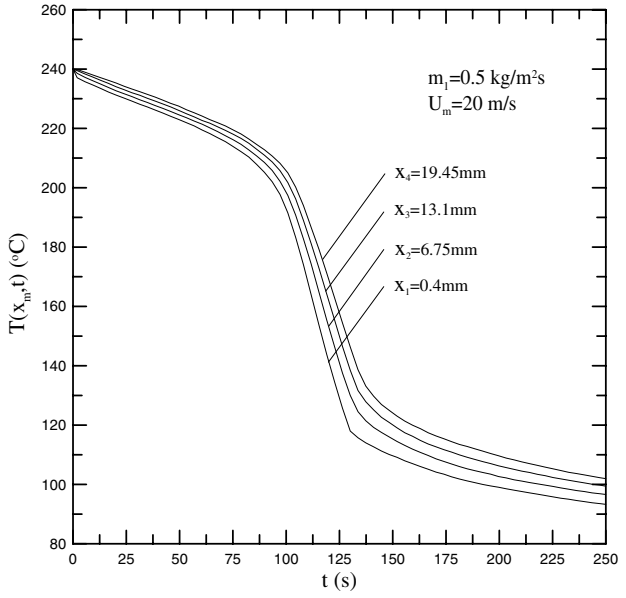

Fig. 9. Experimental temperature data at various measurement locations given by Cui et al. [3] for $m_1 = 0.5\ \text{kg/(m}^2\,\text{s)}$ and $U_m = 20\ \text{m/s}$.

$$T^{\text{mea}}(x_1,t) = \begin{cases} 239.819 - 1.462t + 0.1776t^2 - 1.255\times10^{-2}t^3 \\ \quad +4.81\times10^{-4}t^4 - 1.069\times10^{-5}t^5 \\ \quad +1.413\times10^{-7}t^6 - 1.09\times10^{-9}t^7 \\ \quad +4.513\times10^{-12}t^8 - 7.729\times10^{-15}t^9 \\ \quad \text{for } 0 \leqslant t \leqslant 124\ \text{s} \\ 5.31\times10^5 - 25290t + 532.2t^2 \\ \quad -6.512t^3 + 0.0509t^4 - 2.639\times10^{-4}t^5 \\ \quad +9.079\times10^{-7}t^6 - 1.998\times10^{-9}t^7 \\ \quad +2.553\times10^{-12}t^8 - 1.444\times10^{-15}t^9 \\ \quad \text{for } 124\ \text{s} < t \leqslant 250\ \text{s} \end{cases} \tag{30}$$

$$T^{\text{mea}}(x_2,t) = \begin{cases} 239.801 - 0.535t + 2.105\times10^{-2}t^2 \\ \quad -1.090\times10^{-3}t^3 + 3.677\times10^{-5}t^4 \\ \quad -7.565\times10^{-7}t^5 + 8.896\times10^{-9}t^6 \\ \quad -5.438\times10^{-11}t^7 + 1.302\times10^{-13}t^7, \\ \quad 0 \leqslant t \leqslant 124\ \text{s} \\ 7.178\times10^4 - 2.837t\times10^3 + 48.753t^2 \\ \quad -0.474t^3 + 2.858\times10^{-3}t^4 \\ \quad -1.091\times10^{-5}t^5 + 2.789\times10^{-8}t^6 \\ \quad -3.447\times10^{-11}t^7 + 1.994\times10^{-14}t^8, \\ \quad 124\ \text{s} < t \leqslant 250\ \text{s} \end{cases} \tag{31}$$

$$T^{\text{mea}}(x_3,t) = \begin{cases} 239.988 - 0.272t - 0.01799t^2 - 7.079\times10^{-5}t^3 \\ \quad +1.094\times10^{-5}t^4 - 3.668\times10^{-7}t^5 \\ \quad +5.412\times10^{-9}t^6 - 3.723\times10^{-11}t^7 \\ \quad +9.632\times10^{-14}t^8 \\ \quad \text{for } 0 \leqslant t \leqslant 124\ \text{s} \\ 5880 + 62.333t - 6.352t^2 + 0.123t^3 \\ \quad -1.137\times10^{-3}t^4 + 6.067\times10^{-6}t^5 \\ \quad -1.899\times10^{-8}t^6 + 3.254\times10^{-11}t^7 \\ \quad -2.364\times10^{-14}t^8 \quad \text{for } 124\ \text{s} < t \leqslant 250\ s \end{cases} \tag{32}$$

and

$$T^{\text{mea}}(x_4,t) = \begin{cases} 239.849 + 5.996\times10^{-2}t - 4.058\times10^{-2}t^2 \\ \quad +2.099\times10^{-3}t^3 - 5.274\times10^{-5}t^4 + 6.791\times10^{-7}t^5 \\ \quad -4.298\times10^{-9}t^6 - 1.047\times10^{-11}t^7, \\ \quad 0 \leqslant t \leqslant 124\ \text{s} \\ 5.136\times10^3 - 84.576t - 1.116t^2 + 1.264t^3 - 1.215\times10^{-4}t^4 \\ \quad +5.373\times10^{-7}t^5 - 1.175\times10^{-9}t^6 \\ \quad +1.030\times10^{-12}t^7, \quad 124\ \text{s} < t \leqslant 250\ \text{s} \end{cases} \tag{33}$$

The unknown coefficients $C_j, j = 1, 2, 3$, used to begin the iteration are taken as unity. A second-degree polynomial guess function ($N = 3$) is selected to approximate

the history of the unknown surface temperature $T(0,t)$ on each sub-time interval. Then the nodal temperatures $T_2(t)$ and $T_3(t)$ can be determined from Eq. (12) using the obtained surface temperature $T(0,t)$. Further, the unknown surface heat flux $q(0,t)$ can be obtained from Eq. (25). As shown in Example 1, the deviation of the present estimates is very small for $L = 13.1$ mm and 19.45 mm. Thus $L = 13.1$ mm is used to estimate $T(0,t)$ and $q(0,t)$ in Example 2. Cui et al. [3] also applied the sequential function specification method [7] to estimate the unknown surface heat flux and temperature during spray quenching. Figs. 10 and 11 respectively show the comparisons of $T(0,t)$ and $q(0,t)$ between the present estimates and those given by Cui et al. [3] for $m_1 = 0.5$ kg/m^2 s, $U_m = 20$ m/s, $M = 38$, $x_m = x_1$, $\ell = 0.05$ mm and $L = 13.1$ mm. The results show that the present estimate of the unknown surface temperature $T(0,t)$ agrees well with the estimated result of Cui et al. [3]. However, the present estimate of $q(0,t)$ slightly deviates from the estimated result of Cui et al. [3] for $0 \leqq t \leqq 100$ s. Later, their deviation gradually increases with time for 130 s $\leqq t \leqq$ 80 s. The maximum error between the present estimate and the estimated result of Cui et al. [3] can occur at the final time $t = 180$ s and is up to about 4 times. In addition, the present estimate of $q(0,t)$ is higher than that given by Cui et al. [3] especially for 130 s $\leqq t \leqq 180$ s. The present estimates and the predicted results of Cui et al. [3] both show that the peak values of the surface heat flux $q(0,t)$ occur about at $t = 120$ s. Once the history of the unknown surface heat flux is obtained, $T(0,t)$, $T(x_1,t)$ and $T(x_2,t)$ can be obtained using the present direct scheme. In order to validate the accuracy of $q(0,t)$ further, the comparisons of $T(0,t)$, $T(x_1,t)$ and $T(x_2,t)$ between experimental temperature data given by

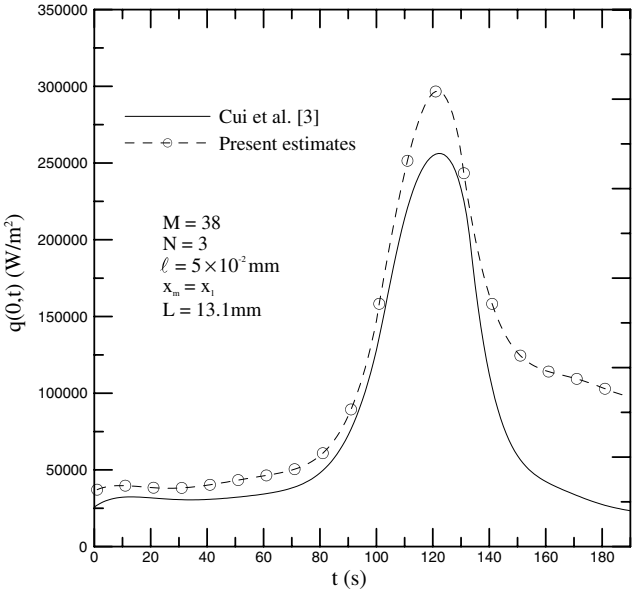

Fig. 11. Comparison of $q(0,t)$ between the present estimates and those given by Cui et al. [3] for $m_1 = 0.5$ kg/(m^2 s), $U_m = 20$ m/s and $L = 13.1$ mm.

Cui et al. [3] and the direct results using two given estimates of $q(0,t)$ are made, as shown in Figs. 12–14. It can be observed from Figs. 12–14 that the present direct results of $T(0,t)$, $T(x_1,t)$ and $T(x_2,t)$ agree well with experimental temperature data given by Cui et al. [3] for the whole time domain $0 \leqq t \leqq 180$ s. However, the deviations between experimental temperature data and the direct results of $T(0,t)$, $T(x_1,t)$ and $T(x_2,t)$ using the estimated result given by Cui et al. [3] is small for $0 \leqq t \leqq 120$ s and gradually increases with time for 120 s $< t \leqq 180$ s. The similar

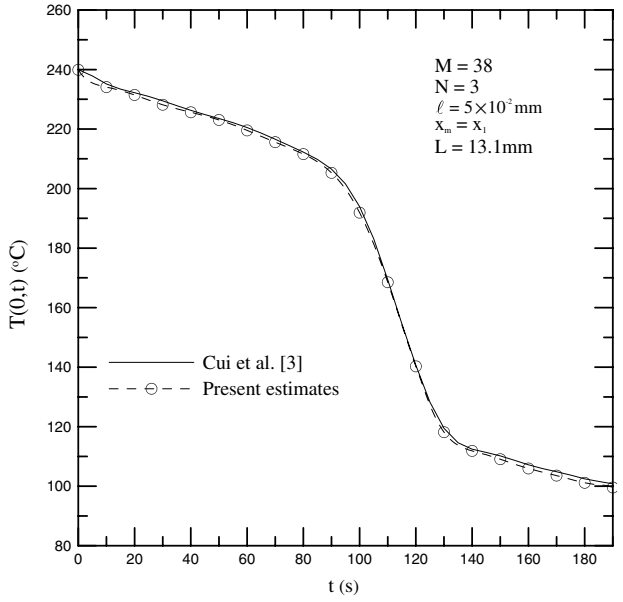

Fig. 10. Comparison of $T(0,t)$ between the present estimates and those given by Cui et al. [3] for $m_1 = 0.5$ kg/(m^2 s), $U_m = 20$ m/s and various L values.

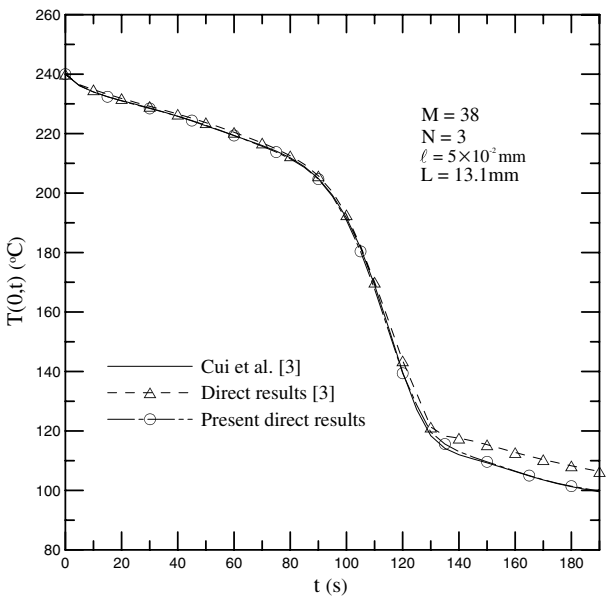

Fig. 12. Comparison of $T(0,t)$ between the direct results using two given estimates of $q(0,t)$ and experimental data given by Cui et al. [3] for $m_1 = 0.5$ kg/(m^2 s), $U_m = 20$ m/s and $L = 13.1$ mm.

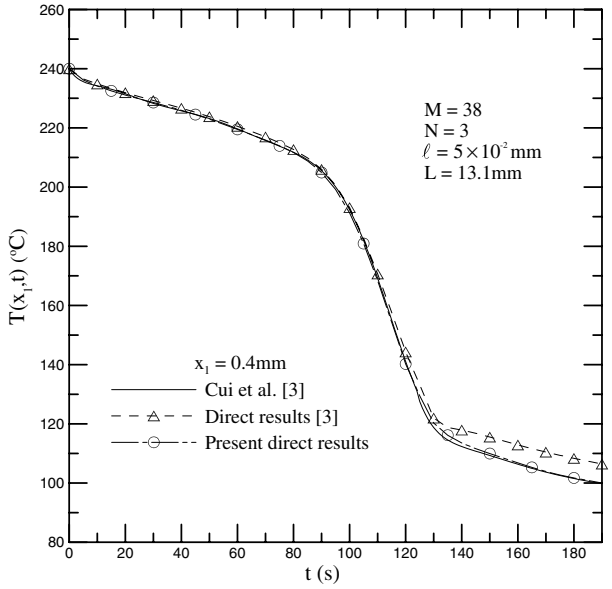

Fig. 13. Comparison of $T(x_1,t)$ between the direct results using two given estimates of $q(0,t)$ and experimental data given by Cui et al. [3] for $m_1 = 0.5$ kg/(m^2 s), $U_m = 20$ m/s and $L = 13.1$ mm.

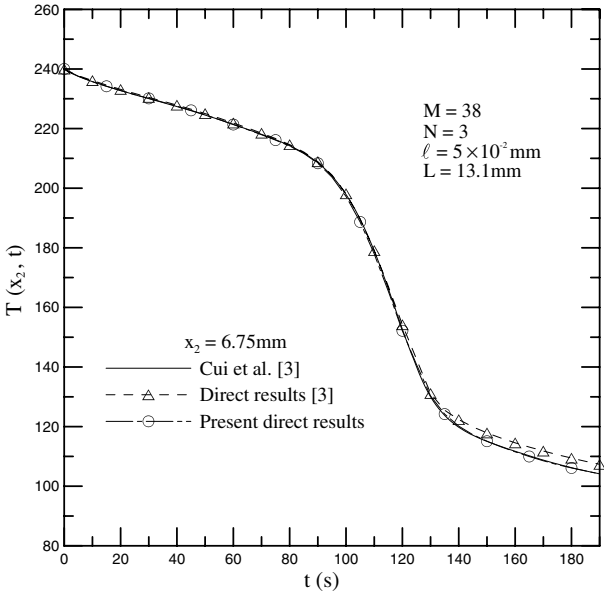

Fig. 14. Comparison of $T(x_2,t)$ between the direct results using two given estimates of $q(0,t)$ and experimental data given by Cui et al. [3] for $m_1 = 0.5$ kg/(m^2 s), $U_m = 20$ m/s and $L = 13.1$ mm.

phenomenon can also be observed from the results in Example 1. This implies that the present inverse scheme can obtain the reliable estimates for the present problems.

Qiao and Chandra [1] and Cui et al. [3] applied the sequential function specification method in conjunction with experimental temperature data to predict the unknown surface heat flux. Their works [1,3] can be useful for validating the accuracy and reliability of an inverse heat conduction scheme. It can be found from Refs. [18,19] that the sequential function specification method can be sensitive to the "thermocouples" locations, number of future times, measurement errors and time step. Moreover, the small dimensionless times should also be based on the distance from the heated surface to the thermocouple nearest the heated surface. However, our previous works [12–15] showed that the estimated results obtained from the present inverse scheme did not deviate from the direct results and were not very sensitive to the measurement time-step and measurement locations even for the problems with measurement errors. This implies that large deviation of the unknown surface heat flux between the present estimates and the estimated results given by Qiao and Chandra [1] and Cui et al. [3] for larger values of time can result from the "thermocouples" locations, number of future times, measurement errors and time step.

5. Conclusions

This study proposes a hybrid inverse scheme involving the Laplace transform and finite-difference methods in conjunction with the least-squares method and experimental temperature data inside the test material to estimate the unknown surface temperature and heat flux of a hot surface during spray cooling. It is found from two different experimental examples that the present estimates of the unknown surface temperature $T(0,t)$ agrees well with experimental temperature data for the whole time domain. However, the present estimates of the unknown surface heat flux $q(0,t)$ slightly deviates from the estimated results of Qiao and Chandra [1] and Cui et al. [3] for the forepart time. Later, their deviation gradually increases with time. In addition, the present direct results obtained from the present scheme at various measurement locations are also in good agreement with experimental temperature data for the whole time domain under the given condition of $q(0,t)$. This implies that the present inverse scheme can obtain the reliable estimates for the present problems.

References

[1] Y.M. Qiao, S. Chandra, Spray cooling enhancements by addition of a surfactant, ASME J. Heat Transfer 120 (1998) 92–98.
[2] W. Jia, H.H. Qiu, Experimental investigation of droplet dynamics and heat transfer in spray cooling, Exp. Thermal Fluid Sci. 27 (2003) 829–838.
[3] Q. Cui, S. Chandra, S. McCahan, The effect of dissolving salts in water sprays used for quenching a hot surface: Part 2 – Spray cooling, ASME J. Heat Transfer 125 (2003) 333–338.
[4] S.S. Hsieh, T.C. Fan, H.H. Tsai, Spray cooling characteristics of water and R-134a. Part II: Transient cooling, Int. J. Heat Mass Transfer 47 (2004) 5713–5724.
[5] E. Hensel, Inverse Theory and Applications for Engineers, Prentice Hall, Englewood Cliffs, NJ, 1991.
[6] M.N. Özisik, Heat Conduction, second ed., Wiley, New York, 1993.
[7] K. Kurpisz, A.J. Nowak, Inverse Thermal Problems, Computational Mechanics Publications, Southampton, UK, 1995.
[8] J. Su, G.F. Hewitt, Inverse heat conduction problem of estimating time-varying heat transfer coefficient, Numer. Heat Transfer A 45 (2004) 777–789.

[9] C.C. Ji, H.Y. Jang, Experimental investigation in inverse heat conduction problem, Numer. Heat Transfer A 34 (1998) 75–91.
[10] S.K. Kim, J.S. Lee, W.I. Lee, A solution method for a nonlinear three-dimensional inverse heat conduction problem using the sequential gradient method combined with cubic-spline function specification, Numer. Heat Transfer B 43 (2003) 43–61.
[11] H.T. Chen, S.M. Chang, Application of the hybrid method to inverse heat conduction problems, Int. J. Heat Mass Transfer 33 (1990) 621–628.
[12] H.T. Chen, S.Y. Lin, L.C. Fang, Estimation of two-sided boundary conditions for two-dimensional inverse heat conduction problems, Int. J. Heat Mass Transfer 45 (2002) 15–23.
[13] H.T. Chen, X.Y. Wu, Y.S. Hsiao, Estimation of surface condition from the theory of dynamic thermal stresses, Int. J. Thermal Sci. 43 (2004) 95–104.
[14] H.T. Chen, X.Y. Wu, Estimation of surface absorptivity in laser surface heating process with experimental data, J. Phys. D: Appl. Phys. 39 (2006) 1141–1148.
[15] H.T. Chen, X.Y. Wu, Estimation of surface conditions for nonlinear inverse heat conduction problems using the hybrid inverse scheme, Numer. Heat Transfer B 51 (2007) 159–178.
[16] G. Honig, U. Hirdes, A method for the numerical inversion of Laplace transforms, J. Comput. Appl. Math. 10 (1984) 113–132.
[17] A.F. Mills, Heat Transfer, second ed., Prentice Hall, Upper Saddle River, NJ, 1999.
[18] J.V. Beck, B. Blackwell, C.R.St. Clair, Inverse Heat Conduction: Ill-Posed Problems, Wiley Interscience, New York, 1985.
[19] A. Behbahani-nia, F. Kowsary, A dual reciprocity BE-based sequential function specification solution method for inverse heat conduction problems, Int. J. Heat Mass Transfer 47 (2004) 1247–1255.